RNA interference–mediated simultaneous down-regulation of urokinase-type plasminogen activator receptor and cathepsin B induces caspase-8–mediated apoptosis in SNB19 human glioma cells

Christopher S. Gondi,[1] Neelima Kandhukuri,[1] Shakuntala Kondraganti,[1] Meena Gujrati,[2] William C. Olivero,[3] Dzung H. Dinh,[3] and Jasti S. Rao[1,3]

[1]Program of Cancer Biology, Department of Biomedical and Therapeutic Sciences and Departments of [2]Pathology and [3]Neurosurgery, University of Illinois College of Medicine at Peoria, Peoria, Illinois

Abstract

The invasive character of gliomas depends on proteolytic cleavage of the surrounding extracellular matrix. Cathepsin B and urokinase-type plasminogen activator receptor (uPAR) together are known to be overexpressed in gliomas and, as such, are attractive targets for gene therapy. In the present study, we used plasmid constructs to induce the RNA interference (RNAi)–mediated down-regulation of uPAR and cathepsin B in SNB19 human glioma cells. We observed that the simultaneous down-regulation of uPAR and cathepsin B induces the up-regulation of proapoptotic genes and initiates a collapse in mitochondrial $\Delta\psi$. Cathepsin B and uPAR down-regulated cells showed increases in the expression of activated caspase-8 and DFF40/caspase-activated DNase. Nuclear translocation of AIF and Fas ligand translocation to the cell membrane were also observed. Ki67 and X-linked inhibitor of apoptosis protein levels decreased, thereby indicating apoptosis. These results suggest the involvement of uPAR-cathepsin B complex on the cell surface and its role in maintaining the viability of SNB19 glioma cells. In conclusion, RNAi-mediated down-regulation of uPAR and cathepsin B initiates a partial extrinsic apoptotic cascade accompanied by the nuclear translocation of AIF. Our study shows the potential of RNAi-mediated down-regulation of uPAR and cathepsin B in developing new therapeutics for gliomas. [Mol Cancer Ther 2006; 5(12):3197–208]

Introduction

Malignant gliomas are characterized by invasive and infiltrative behavior, which involves the destruction of normal brain tissue (1, 2). Strategies to treat infiltrating gliomas, such as chemotherapy and gene therapy, have remained largely unsuccessful. The infiltrative nature of gliomas can be attributed largely to proteases, which include serine proteases, metalloproteases, and cysteine proteases. Our previous work and that of others strongly suggest a relationship between urokinase-type plasminogen activator receptor (uPAR) and cathepsin B expression and the infiltrative phenotype of gliomas (3–6). Many researchers have focused on targeting these proteases to control or prevent metastasis. Proteases are integral for several, normal cellular processes, including matrix adhesion, tissue repair, and remodeling (7, 8). During cancer cell invasion, these proteases, either singly or in combination, function to degrade the extracellular matrix, thereby facilitating metastasis. uPA, a serine protease, mediates the conversion of plasminogen to plasmin, a broad-spectrum protease. uPA is secreted as a pro-form, and its activation is mediated by its receptor uPAR. Cathepsin B has also been implicated in the activation of uPA and various matrix metalloproteases (9). Notably, cathepsin B plays a dual role by being both proapoptotic and antiapoptotic, depending on different conditions (10–13). In gliomas, cathepsin B is involved in extracellular matrix degradation and hence is an attractive target for antimetastatic therapy.

Malignant gliomas are characterized by the invasive infiltration and destruction of normal brain tissue surrounding the glioma tumor mass. Our earlier work and that of others have indicated a direct correlation of cathepsin B with infiltrative gliomas. Results with antisense cathepsin B and sense cystatin c stable cells of SNB19 showed that the cells were less invasive and failed to establish *ex vivo* tumors (9, 14–17). RNA interference (RNAi) technology has emerged as a fast-growing and efficient tool in silencing gene expression. Our earlier work showed the use of RNAi in efficiently targeting uPAR and cathepsin B (18). We have previously shown that the use of cytomegalovirus promoter–based plasmid vectors to drive the production of hairpin RNA molecules targeting uPAR and cathepsin B effectively down-regulates uPAR and cathepsin B mRNA and protein. The down-regulation of

Received 12/19/05; revised 8/29/06; accepted 10/18/06.

Grant support: National Cancer Institute grants CA 75557, CA 92393, CA 95058, and CA 116708; National Institute of Neurological Disorders and Stroke grant NS47699; Caterpillar, Inc., Peoria, IL (J.S. Rao); and OSF Saint Francis, Inc., Peoria, IL (J.S. Rao).

The costs of publication of this article were defrayed in part by the payment of page charges. This article must therefore be hereby marked advertisement in accordance with 18 U.S.C. Section 1734 solely to indicate this fact.

Requests for reprints: Jasti S. Rao, Program of Cancer Biology, Department of Biomedical and Therapeutic Sciences, University of Illinois College of Medicine at Peoria, One Illini Drive, Peoria, IL 61605. Phone: 309-671-3445. E-mail: jsrao@uic.edu

doi:10.1158/1535-7163.MCT-05-0531

uPAR and cathepsin B retarded invasion and migration as well as inhibition of the development and growth of intracranial tumors. Furthermore, we have also previously observed the down-regulation of phospho–focal adhesion kinase and phospho–extracellular signal-regulated kinase 1/2, both prosurvival molecules, and the retardation of growth in general. In this study, we have attempted to explore the possible mechanisms that are involved in retardation of tumor cell growth, migration, invasion, and intracranial tumor establishment.

Materials and Methods

Small Interfering RNA Vector Construction

RNAi vectors were based on the PCDNA 3 backbone driven by a cytomegalovirus promoter as described earlier (18). uPAR sequence from +77 to +98 was used as the target sequence, and, for convenience, a self-complimentary oligo was used. The uPAR sequence was 21 bases in length with a 9-base loop region and *Bam*HI sites incorporated at the ends (GATCCTACAGCAGTGGAGAGCGATTATATATAATAATCGCTCTCCACTGCTGTAG). The oligo was self-annealed in 6× SSC per standard protocols and ligated onto the *Bam*HI site of a pcDNA-3 vector plasmid. Similarly, a cathepsin B complimentary sequence from +732 to +753 (TCGAGGTGGCCTCTATGAATCCCAATATATAATTGGGATTCATAGAGGCCACC) with *Xho*I sites incorporated at the ends was ligated into the *Xho*I site of the vector containing the small interfering RNA (siRNA) sequence for uPAR. This finally resulted in a siRNA expression plasmid for cathepsin B and uPAR designated as pUC. Single siRNA expression vectors for uPAR (puPAR) and cathepsin B (pCath B) were also constructed. The orientation of either insert in the single or bicistronic construct was not relevant because the oligos were self-complimentary and had bilateral symmetry. BGH polyadenylate terminator served as a stop signal for RNA synthesis for all three constructs.

Antibodies

Antibodies targeting uPAR (R&D Systems, Minneapolis, MN) and cathepsin B (Athens Research Technologies, Athens, GA) were used to determine the presence or absence of these molecules on the cell surface and to determine the induction of apoptosis by interfering with these molecules in live cells. siRNA-mediated down-regulation of uPAR and cathepsin B would cause a reduction of the molar concentration of these molecules on the cell surface, whereas antibodies would only interfere with the molecular interactions of uPAR and cathepsin B. Caspase-9, caspase-8, caspase-3, and X-linked inhibitor of apoptosis protein (XIAP) were obtained from Cell Signaling Technologies (Danvers, MA). Fas ligand (FasL), Ki67, and glyceraldehyde-3-phosphate dehydrogenase were obtained from Abcam (Cambridge, MA). Cytochrome *c* was obtained from BD Biosciences (San Jose, CA); caspase-activated DNase (CAD) and AIF were obtained from Sigma-Aldrich (St. Louis, MO); and cleaved poly(ADP-ribose) polymerase (PARP) was obtained from Oncogene Research Products (San Diego, CA).

Cell Culture and Transfection Conditions

The SNB19 (or SNB19 GFP) cell line, established from a human high-grade glioma, was used for this study. Cells were grown in DMEM/F12 media (1:1, v/v) supplemented with 10% FCS in a humidified atmosphere containing 5% CO_2 at 37°C. SNB19 cells were transfected with plasmid constructs (empty vector, puPAR, pCath B, or pUC) using LipofectAMINE as per manufacturer's instructions (Life Technologies, Rockville, MD).

Isolation of Mitochondrial and Cytosolic Cell Fractions

SNB19 cells were transfected with either mock, empty vector, puPAR, pCath B, or pUC, or with antibodies for uPAR, cathepsin B, or both, and cultured for 48 h. At the end of incubation, cells were harvested, washed twice, and resuspended in 0.5 g/mL osmotic buffer [10 mmol/L $NaPO_4$, 1.35 mol/L sorbitol, 1 mmol/L EDTA, 2.5 mmol/L DTT (pH 7.5)] with Zymolyase 20T (Associates of Cape Cod, Inc., East Falmouth, MA) added to a final concentration of 3 mg/g cells. Cells were then incubated at 30°C with gentle shaking for 5 min, after which the cells were resuspended in lysis buffer [0.6 mol/L mannitol, 2 mmol/L EDTA (pH 7)]. Protease inhibitors phenylmethylsulfonyl fluoride and aprotinin were added to the lysis buffer immediately before cell lysis. Cells were lysed by vigorous vortexing. Cellular debris was removed by centrifugation (1,900 × *g* for 5 min). The supernatant containing both the mitochondrial and cytosolic fractions was then centrifuged (12,100 × *g* for 10 min) to pellet the mitochondria. The resulting supernatant, designated as the cytosolic fraction, was frozen at −80°C or used for Western blotting. The mitochondrial pellet was washed once in 0.6 mol/L mannitol, 2 mmol/L EDTA (pH 7) and centrifuged at 1,651 × *g* for 5 min to pellet any remaining debris. The supernatant containing the mitochondria was then pelleted by centrifugation (23,000 × *g* for 10 min), resuspended in 10 mmol/L $NaPO_4$ (pH 7) to a final concentration of ~5 to 10 μg/μL, and frozen at −80°C or used as such. Intact mitochondria were lysed in lysis buffer [150 mmol/L NaCl, 50 mmol/L Tris-HCl, 2 mmol/L EDTA, 1% NP40 (pH 7.4)] and Western blotted.

Western Blotting

SNB19 cells were transfected with either mock, empty vector, puPAR, pCath B, or pUC, or with antibodies for uPAR, cathepsin B, or both, and cultured 48 h. At the end of incubation, cells were harvested, washed twice with cold PBS, and lysed in buffer [150 mmol/L NaCl, 50 mmol/L Tris-HCl, 2 mmol/L EDTA, 1% NP40 (pH 7.4)] containing protease inhibitors. Equal amounts of protein (30 μg per lane) from supernatants or cells were electrophoresed under nonreducing conditions on 10% acrylamide gels. After SDS-PAGE, proteins were transferred to a polyvinylidene difluoride membrane (Bio-Rad, Richmond, CA). To block nonspecific binding, the membrane was incubated for 2 h in PBS with 0.1% Tween 20 (T-PBS) containing 5% nonfat skim milk for 2 h. Subsequently, the membrane was incubated for 2 h with antibody against cathepsin B, uPAR, CAD, caspase-8, caspase-3, FasL, XIAP, Ki67, caspase-9, and cleaved PARP, respectively,

in T-PBS + 5% nonfat milk. After washing in T-PBS, protein on the membrane was visualized using the ECL detection kit with a peroxidase-labeled anti-rabbit or anti-mouse antibody (Amersham Pharmacia Biotech, Amersham, United Kingdom) as per manufacturer's instructions. For loading control, the membranes were stripped and probed with monoclonal antibodies for glyceraldehyde-3-phosphate dehydrogenase per standard protocol. Levels of caspase-8– and caspase-3–activated forms were also determined.

Matrigel Invasion Assay

The *in vitro* invasiveness of SNB19 cells in the presence of the vector expressing siRNA for cathepsin B and uPAR was assessed using a modified Boyden chamber assay. SNB19 cells were transfected with mock, empty vector, or a vector expressing siRNA for cathepsin B and uPAR for 48 h. Cells (1×10^6) were suspended in 600 μL of serum-free medium supplemented with 0.2% bovine serum albumin and placed in the upper compartment of the Transwell chambers (Corning Costar Fischer Scientific, Pittsburgh, PA) coated with Matrigel (0.7 mg/mL). The lower compartment of the chamber was filled with 200 μL of serum-free medium, and the cells were allowed to migrate for 24 h. After incubation, the cells were fixed and stained with Hema-3 and quantified as previously described (19).

Visualization of Mitochondrial Permeability Transition

SNB19 cells were cultured to 50% confluence and transfected with control, empty vector, scrambled vector, puPAR, pCath B, or pUC, or with antibodies for uPAR, cathepsin B, or both. Seventy-two hours after transfection or antibody treatment, the cells were trypsinized and resuspended in serum-free media containing 5,5′,6,6′-tetrachloro-1,1′3,3′-tetraethylbenzamidazolocarbocyanin iodide (JC-1) using the MitoPT kit. Fifteen to 20 min after incubation at 37°C, the cells were fixed and observed for red/green fluorescence. Cells were counted using a flow cytometer for red or green fluorescence, and results were quantified.

Determination of Translocation of Phosphatidylserine to the Cell Surface

To determine weather pUC-transfected cells were committed to the apoptotic pathway, SNB19 cells were transfected with control, empty vector, scrambled vector, puPAR, pCath B, or pUC, and the cell surface translocation of phosphatidylserine was determined by staining with FITC-conjugated Annexin V (Biovision, Mountain View, CA). The Annexin V apoptosis detection kit is based on the observation that after initiating apoptosis, cells translocate the membrane phosphatidylserine from the inner face of the plasma membrane to the outer surface. Once on the cell surface, phosphatidylserine is detected by staining with a FITC conjugate of Annexin V. Briefly, SNB19 cells were grown in chamber slides and transfected with control, empty vector, scrambled vector, puPAR, pCath B, or pUC in three sets. Translocation of phosphatidylserine to the outer surface of the cell membrane was determined at 60, 66, and 72 h after transfection as per manufacturer's instructions. Cells were incubated with Annexin V-FITC before fixation because any cell membrane disruption would cause nonspecific binding of Annexin V to phosphatidylserine on the inner surface of the cell membrane, and the cells were then washed with PBS and fixed in 2% formaldehyde before visualization. Cells were observed under a fluorescence microscope, using standard filter set for FITC. Cells that have bound Annexin V-FITC were observed for green fluorescence in the plasma membrane. The fluorescent cells were counted and quantified as percentage of total cells as determined by phase-contrast microscopy.

Caspase Activity Assay

Caspase assay was done using colorimetric assay kits as per manufacturer's instructions. SNB19 cells were transfected with control, empty vector, scrambled vector, puPAR, pCath B, or pUC, or with antibodies for uPAR, cathepsin B, or both, with or without appropriate inhibitors as controls. The activation of caspase-3 and caspase-8 was determined colorimetrically. The Caspase-8 Colorimetric Assay kit (Sigma-Aldrich) is based on the hydrolysis of the peptide substrate Acetyl-Ile-Glu-Thr-Asp-*p*-nitroaniline (Ac-IETD-*p*-NA) by caspase-8 that results in the release of a *p*-nitroaniline (*p*-NA) moiety. The *p*-NA was measured colorimetrically at 405 nm. The caspase-3 colorimetric assay kit is based on hydrolysis of acetyl-Asp-Glu-Val-Asp-*p*-nitroanilide (Ac-DEVD-*p*-NA) by caspase-3 that results in the release of a *p*-nitroaniline (*p*-NA) moiety. The *p*-NA was measured colorimetrically at 405 nm, similar to the caspase-8 assay. The assays were done as per manufacturer's instructions, using appropriate controls with and without inhibitors. The results were quantified and graphically represented.

Immunocytochemistry

SNB19 cells (1×10^4) were seeded on vitronectin-coated eight-well chamber slides, incubated for 24 h, and transfected with either empty vector/scrambled vector, puPAR, pCath B, or pUC, or with antibodies for uPAR, cathepsin B, or both. After 72 h, cells were fixed with 3.7% formaldehyde and incubated with 1% bovine serum albumin in PBS at room temperature for 1 h for blocking. After the slides were washed with PBS, either IgG anti-AIF (rabbit) or IgG anti-FasL (mouse) was added at a concentration of 1:200. The slides were incubated overnight at 4°C and washed thrice with PBS to remove excess primary antibody. Cells were then incubated with anti-mouse FITC conjugate or anti-rabbit horseradish peroxidase–conjugated IgG (1:500 dilution) for 1 h at room temperature. The slides were then washed thrice and covered with glass coverslips, and fluorescent photomicrographs were obtained for FITC. For detection of AIF, the slides were treated with horseradish peroxidase substrate 3,3′-diaminobenzidine as per standard protocol and photomicrographed using white light. 4′,6-Diamidino-2-phenylindole (DAPI) images were obtained where appropriate.

Visualization of Nuclear Fragmentation

SNB19 cells (1×10^4) were seeded on vitronectin-coated eight-well chamber slides, incubated for 24 h, and transfected with empty vector/scrambled vector, puPAR,

pCath B, or pUC. After 48 h, cells were fixed with 3.7% formaldehyde for 20 min at room temperature. The cells were then gently washed in PBS thrice and incubated in 1 μg/mL RNase in PBS for 30 min. The cells were washed again gently and covered with a coverslip mounted in DAPI-containing mounting media. DAPI fluorescence was visualized using a fluorescent microscope.

Cell Cycle Analysis

SNB19 cells (2×10^6) were seeded on vitronectin-coated plates and were transfected with either mock, empty vector, puPAR, pCath B, or pUC, or treated with antibodies for uPAR, cathepsin B, or both, and cultured for 48 h. Cells were then trypsinized and treated with 50 μg/mL propidium iodide + 0.001% RNase A solution as per standard protocol. The cells were sorted on a fluorescence-activated cell sorter and quantified (10,000 cells sorted).

Results

pUC Plasmid Expressing siRNA-Targeting uPAR and Cathepsin B Decreases uPAR and Cathepsin B Protein Levels

RNAi targeted against proteolytic degradation could be an important intervention to prevent cancer cell invasion. Cathepsin B and uPAR have been shown to play significant roles in extracellular matrix degradation. Transfection of SNB19 cells with the vector expressing siRNA for cathepsin B and uPAR (pUC) strongly inhibited the expression of both proteins compared with empty vector and scrambled vector (Fig. 1A). Glyceraldehyde-3-phosphate dehydrogenase levels showed equal quantities of protein were loaded (Fig. 1A). Quantitative analysis of cathepsin B and uPAR bands by densitometry revealed a significant ($P < 0.001$) decrease in cathepsin B (14- to 16-fold) and uPAR (10- to 12-fold) protein in pUC-transfected cells compared with controls (Fig. 1B). Cells transfected with puPAR and pCath B vectors also decreased uPAR and cathepsin B protein levels, respectively (Fig. 1A).

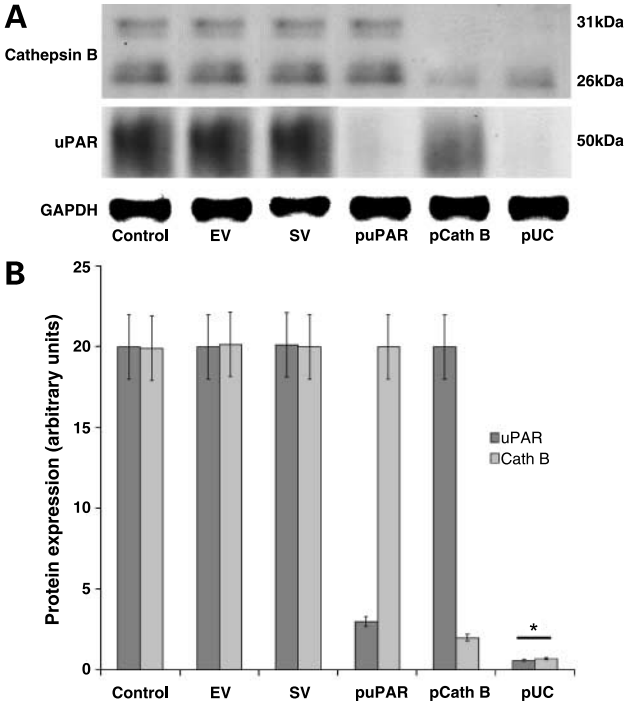

Figure 1. **A,** Western blot analysis of uPAR and cathepsin B. SNB19 cells were transfected with mock, empty vector, puPAR, pCath B, or pUC for 48 h. At the end of incubation, cells were harvested, washed twice with cold PBS, and lysed in buffer [150 mmol/L NaCl, 50 mmol/L Tris-HCl, 2 mmol/L EDTA, 1% NP40 (pH 7.4)] containing protease inhibitors. Equal amounts of protein (30 μg per lane) from supernatants, or cells were electrophoresed under nonreducing conditions on 10% acrylamide gels. After SDS-PAGE, proteins were transferred to a polyvinylidene difluoride membrane (Bio-Rad). To block nonspecific binding, the membrane was incubated for 2 h in PBS with 0.1% Tween 20 (T-PBS) containing 5% nonfat skim milk. Subsequently, the membrane was incubated for 2 h with antibody against cathepsin B and uPAR, in T-PBS + 5% nonfat milk. After washing in T-PBS, protein on the membrane was visualized using the ECL detection kit with a peroxidase-labeled anti-rabbit or anti-mouse antibody (Amersham Pharmacia Biotech) as per manufacturer's instructions. For loading control, the membranes were stripped and probed with monoclonal antibodies for GAPDH per standard protocol. **B,** quantitative analysis of cathepsin B and uPAR bands by densitometry.

RNAi-Mediated Down-regulation of uPAR and Cathepsin B Increases the Expression Levels of Proapoptotic Genes

SNB19 cells were transfected with mock, empty vector, scrambled vector, puPAR, pCath B, or pUC, or with antibodies for uPAR, cathepsin B, or both, and cultured for 48 h. At the end of incubation, cells were harvested, washed twice with cold PBS and lysed in buffer [150 mmol/L NaCl, 50 mmol/L Tris-HCl, 2 mmol/L EDTA, 1% NP40 (pH 7.4)], containing protease inhibitors. Equal amounts of protein (30 μg per lane) were loaded on polyacrylamide gels and electrophoresed as described earlier. Western blots were immunoprobed for caspase-8, caspase-3, caspase-9, CAD, FasL, XIAP, Ki67, and cleaved PARP. Cytoplasmic and mitochondrial protein fractions were immunoprobed for cytochrome *c*. Figure 2A shows the Western blot analysis of SNB19 cells transfected with puPAR, pCath B, and pUC. An observable increase in the levels of activated caspase-9 was seen in pUC-transfected cells. Cytoplasmic levels of cytochrome *c* showed an increase in pUC-transfected cells with detected levels in puPAR- and pCath B–transfected cells. Levels of CAD were also observed in puPAR-, pCath B–, and pUC-transfected cells. No change in the expression levels of FasL was observed. The level of XIAP, an inhibitor of apoptosis, was not detected in pUC-transfected cells. PARP cleavage was observed, and a corresponding decrease in the levels of Ki67 was seen. No change in the total levels of AIF was observed. Similarly, Western blot analysis was done with SNB19 cells treated with antibodies targeting uPAR, cathepsin B, or together. An Isomatch antibody was used as control. In the antibody-treated cells, no change in the levels of caspase-9, FasL, cleaved PARP, XIAP, or Ki67 was observed (Fig. 2B). Similar to the RNAi-transfected cells, no change in the levels of AIF was observed. From the colorimetric caspase-8 (Fig. 2C) and caspase-3

(Fig. 2D) assays, it was observed that the levels of activated caspase-8 in puPAR-, pCath B–, and pUC-treated cells increased. The levels of activated caspase-8 in pUC-treated cells were comparable with the positive controls. Cells treated with antibodies targeting uPAR and cathepsin B, either singly or in combination, did not show any evidence of caspase-8 activation and were comparable with blank control (Fig. 2C). From the caspase-3 colorimetric assay, it was observed that RNAi transfection and antibody treatment did not induce the activation of caspase-3 (Fig. 2D). Western blots for caspase-8 and caspase-3 were also done to visualize the activated forms under various treatment conditions with either RNAi or antibodies. SNB19 cells transfected with puPAR, pCath B, and pUC showed increase in the activation of caspase-8, whereas no activation of caspase-3 was observed (Fig. 2E). SNB19 cells treated with antibodies targeting uPAR and cathepsin B, either singly or in combination, did not show the activation of either caspase-3 or caspase-8 (Fig. 2F).

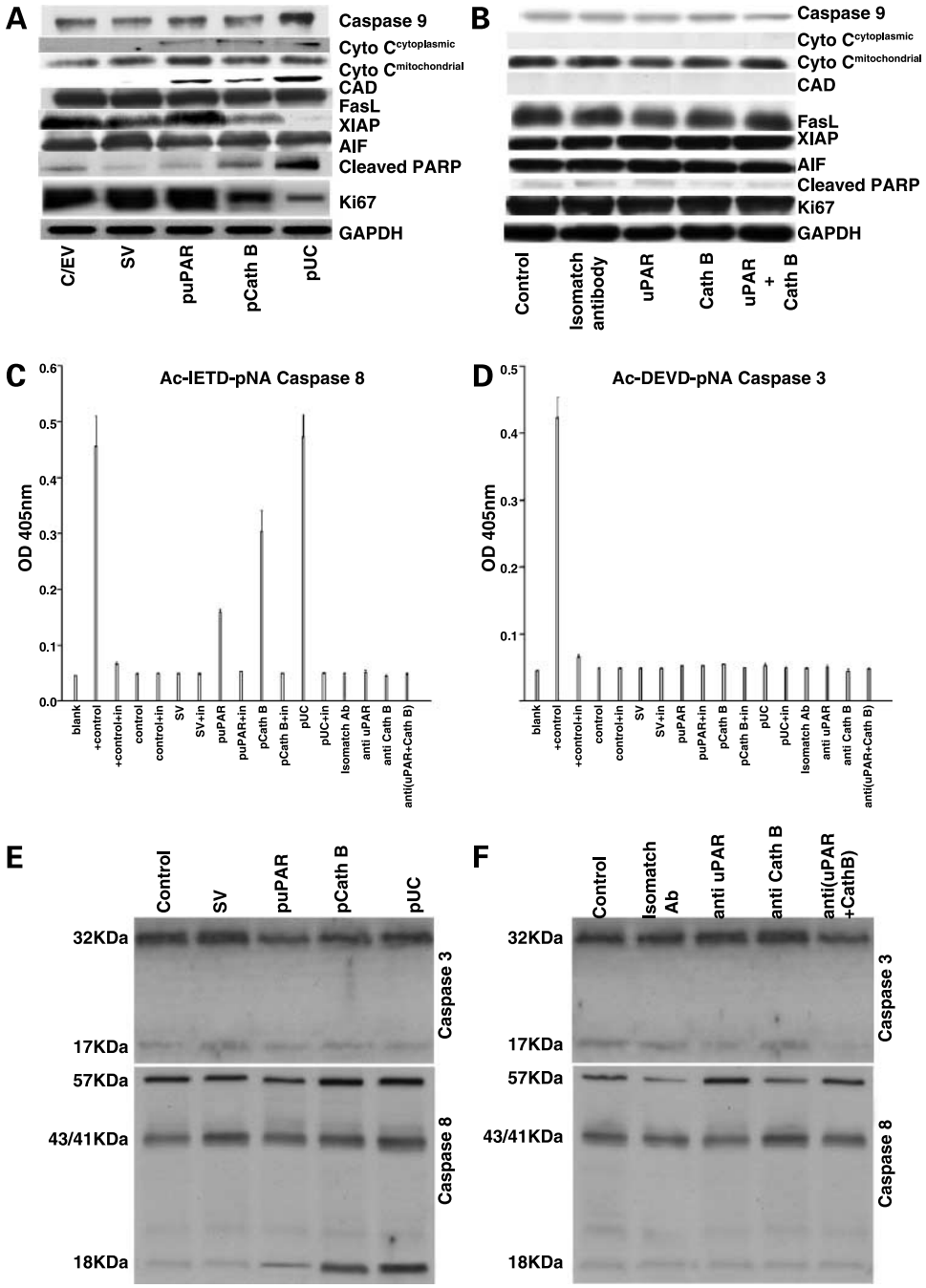

Figure 2. Western blot analysis and caspase-8 and caspase-3 activation assay of SNB19 cells either transfected with mock, empty vector, puPAR, pCath B, or pUC, or treated with antibodies for uPAR, cathepsin B, or both. Western blots from cells transfected with control/empty vector (*EV*), scrambled vector (*SV*), puPAR, pCath B, and pUC were immunoprobed with antibodies for CAD, caspase-9, FasL, XIAP, Ki67, and cleaved PARP in T-PBS + 5% nonfat milk for 2 h. **A,** proteins fractionated into cytoplasmic and mitochondrial fractions (see Materials and Methods) were also run on SDS-PAGE and immunoprobed for cytochrome *c*. Western blots from cells treated with control or antibodies for uPAR, cathepsin B, or both were immunoprobed with antibodies for CAD, caspase-9, FasL, XIAP, Ki67, and cleaved PARP, respectively, in T-PBS + 5% nonfat milk for 2 h. **B,** proteins fractionated into cytoplasmic and mitochondrial fractions (see Materials and Methods) were also run on SDS-PAGE and immunoprobed for cytochrome *c*. After washing in T-PBS, proteins on the membrane were visualized using the ECL detection kit with a peroxidase-labeled anti-rabbit or anti-mouse antibody (Amersham Pharmacia Biotech) per manufacturer's instructions. For loading control, the membranes were stripped and probed with monoclonal antibodies for glyceraldehyde-3-phosphate dehydrogenase (*GAPDH*) per standard protocol. Caspase-8 and caspase-3 activation was assayed using a colorimetrically assay kit at 405 nm for release of *p*-NA as per manufacturer's instructions (**C** and **D**). Western blots from cells transfected with control/empty vector, scrambled vector, puPAR, pCath B, and pUC were immunoprobed with antibodies for caspase-8 and caspase-3 to visualize activated forms (**E** and **F**).

Transfection of SNB19 Cells with a Plasmid Expressing siRNA-Targeting uPAR and Cathepsin B Induces a Collapse in Mitochondrial $\Delta\psi$, Translocation of AIF to the Nucleus, and Nuclear Fragmentation

SNB19 cells were transfected with mock, empty vector, puPAR, pCath B, or pUC, or treated with antibodies for uPAR, cathepsin B, or both. JC-1 dye was used to observe cell fluorescence. Red fluorescence indicates intact mitochondria, whereas green fluorescence indicates a collapse in mitochondrial $\Delta\psi$. Figure 3A shows that pUC transfection of SNB19 cells induced mitochondrial $\Delta\psi$ collapse. JC-1 dye fluorescence was quantified using a flow cytometer (Fig. 3C). SNB19 cells treated with antibodies for uPAR and cathepsin B, either singly or together, did not show any change in mitochondrial permeability (data not shown). Transfected and antibody-treated SNB19 cells were also immunoprobed for AIF. Cells transfected with pUC showed the translocation of AIF to the nucleus (Fig. 3B), whereas no change was observed in cells treated with antibodies (data not shown). Quantification of AIF translocation to the nucleus was determined based on time and the percentage of cells showing nuclear translocation (Fig. 3D). Forty-eight hours after transfection, 85% of pUC-transfected cells showed nuclear translocation of AIF ($P = 0.05$). SNB19 cells transfected with mock, empty vector, puPAR, pCath B, or pUC, or treated with antibodies for uPAR, cathepsin B, or both, were assayed for their ability to invade Matrigel using the standard Matrigel invasion assay. From the Matrigel invasion assay, it was observed that the uPAR and cathepsin B antibody treatment and pUC RNAi transfection retarded the invasive ability of SNB19 cells by 87 ± 3% and 82 ± 7%, respectively. Antibodies targeting uPAR and cathepsin B when treated singly retarded invasion with almost equal efficiency (73 ± 2%) and were more efficient than puPAR-transfected (48 ± 4%) or pCath B–transfected (28 ± 8%)

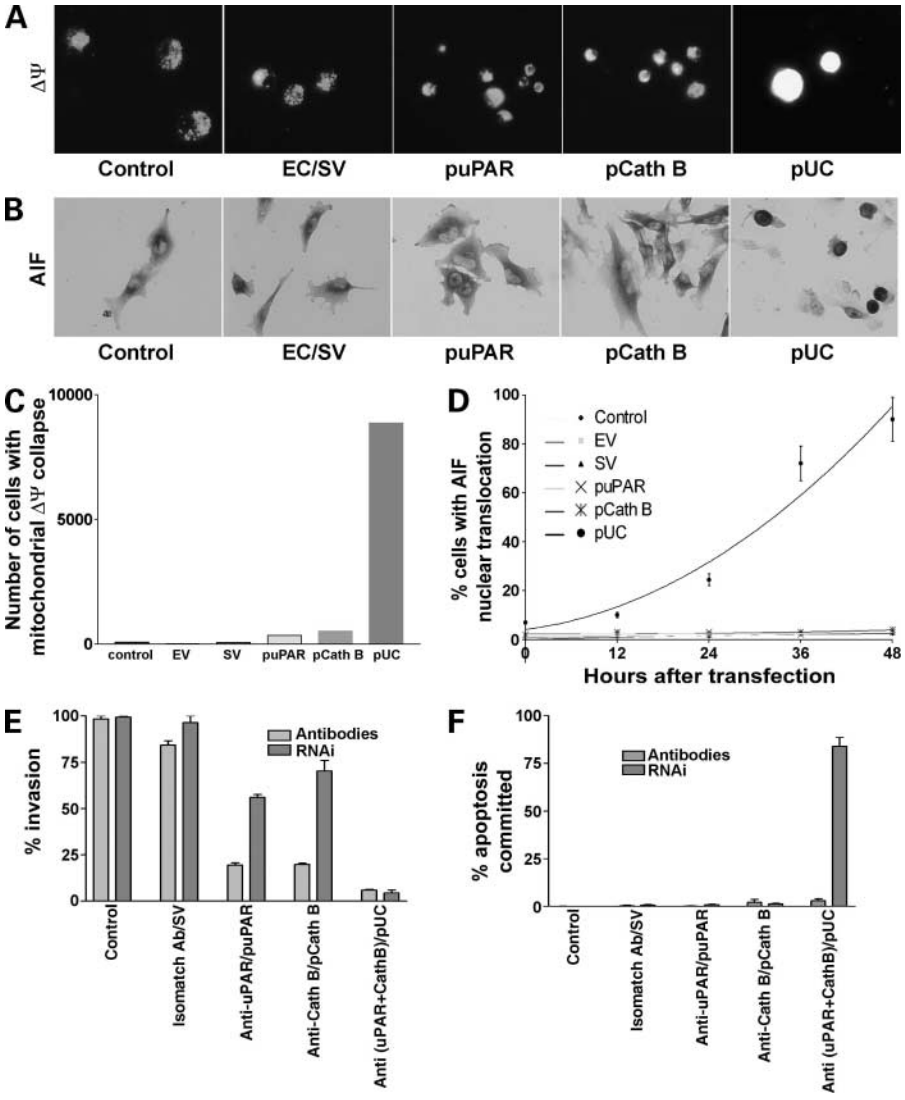

Figure 3. Immunocytochemical analysis of mitochondrial $\Delta\psi$ collapse, AIF nuclear translocation, Matrigel invasion, and induction of apoptosis. SNB19 cells were cultured to 50% confluence and transfected with control, empty vector, scrambled vector, puPAR, pCath B, or pUC. Seventy-two hours later, cells were processed using the MitoPT kit. **A,** 15 to 20 min after incubation at 37°C, the cells were fixed and observed for red/green fluorescence. **C,** cells were counted using a flow cytometer for red or green fluorescence, and results were quantified. SNB19 cells (1×10^4) were seeded on vitronectin-coated eight-well chamber slides, incubated for 24 h, and transfected with empty vector/scrambled vector, puPAR, pCath B, or pUC. After 72 h, cells were fixed with 3.7% formaldehyde and incubated with 1% bovine serum albumin in PBS at room temperature for 1 h for blocking. After the slides were washed with PBS, IgG anti-AIF (rabbit) was added at a concentration of 1:200. The slides were incubated at 4°C overnight and washed three times with PBS to remove excess primary antibody. Cells were then incubated with anti-rabbit horseradish peroxidase–conjugated IgG (1:500 dilution) for 1 h at room temperature. The slides were then washed three times in PBS. **B,** for the detection of AIF, the slides were treated with horseradish peroxidase substrate DAB per standard protocol and photomicrographed using white light. **D,** the results were quantified and graphically represented. **E,** plasmid-transfected and antibody-treated cells were also assayed using the standard Matrigel invasion assay. **F,** SNB19 cells showing nuclear fragmentation were also determined and quantified as a percentage of apoptotic cells and graphically represented.

cells (Fig. 3E). Antibody treatments did not show any significant induction of nuclear fragmentation indicative of apoptosis, whereas SNB19 cells transfected with pUC showed 89 ± 10% induction of apoptosis (Fig. 3F).

Transfection of SNB19 Cells with a Plasmid Expressing siRNA-Targeting uPAR and Cathepsin B Induces the Accumulation of FasL on the Cell Surface, Induces Nuclear Condensation/Fragmentation, and Increases the Sub-G_1 Population of Cells

SNB19 cells were transfected with either mock, empty vector, puPAR, pCath B, or pUC, or treated with antibodies for uPAR, cathepsin B, or both, and cultured for 48 h. Cells were then fixed with 3.7% formaldehyde and incubated with 1% bovine serum albumin in PBS at room temperature for 1 h for blocking. The slides were then washed with PBS, after which IgG anti-FasL (mouse) was added at a concentration of 1:200. The slides were incubated at 4°C overnight and washed thrice with PBS to remove excess primary antibody. Cells were then incubated with anti-mouse FITC conjugate IgG (1:500 dilution) for 1 h at room temperature. The slides were then washed thrice and covered with glass coverslips, and fluorescent photomicrographs were obtained for FITC. DAPI images were obtained where appropriate. Figure 4A shows pUC-transfected cells with localization of FasL seen on the cell surface when compared with the controls, puPAR-, or pCath B–transfected cells. No change was observed in cells treated with antibodies for uPAR, cathepsin B, or both (Fig. 3F). SNB19 cells were transfected with control, empty vector, scrambled vector, puPAR, pCath B, or pUC, or with antibodies for uPAR, cathepsin B, or both, and cultured for 48 h. Cells were then fixed with 3.7% formaldehyde and mounted in DAPI-containing mounting media. Fluorescent images were obtained to visualize nuclear morphology. pUC-transfected cells showed nuclear condensation and fragmentation (Fig. 4B). Control, empty vector/scrambled vector–, puPAR-, and pCath B–transfected cells did not show any change in nuclear morphology. Quantitative analysis of the percentage of cells showing nuclear fragmentation and condensation revealed >35% cells with fragmented or condensed nuclei in pUC-transfected cells (Fig. 4C). SNB19 cells treated with uPAR or cathepsin B antibodies, alone or in combination, did not show any nuclear fragmentation or condensation and were similar to controls (data not shown). SNB19 cells (2×10^6) were seeded on vitronectin-coated plates and were transfected with mock, empty vector, puPAR, pCath B, or pUC, or treated with antibodies for uPAR, cathepsin B, or both, and cultured for 48 h. Cells were then trypsinized and treated with 50 μg/mL propidium iodide + 0.001% RNase A solution per standard protocols. Cells were sorted in a fluorescence-activated cell sorter and quantified (10,000 cells sorted). Figure 4D shows the increase in the sub-G_1 population of cells in pUC-transfected cells. A small fraction of cells also were arrested in the G_0-G_1 phase. Cells treated with antibodies against uPAR and cathepsin B was similar to controls.

Transfection of SNB19 Cells with a Plasmid Expressing siRNA-Targeting uPAR and Cathepsin B Induces the Translocation of Membrane Phosphatidylserine from the Inner Surface to the Outer Surface of the Cell Membrane

To determine whether pUC-transfected cells were committed to the apoptotic pathway, SNB19 cells were transfected with control, empty vector, scrambled vector, puPAR, pCath B, or pUC, and the cell surface translocation of phosphatidylserine was determined by staining with FITC-conjugated Annexin V as described in Materials and Methods. Figure 5A shows the presence of phosphatidylserine on the outer membrane surface in cells that are committed to the apoptotic pathway by staining with FITC-conjugated Annexin V. It is observed that 60 h after transfection of SNB19 cells with pUC, >40% cells showed outer membrane translocation of phosphatidylserine. The translocation of phosphatidylserine increased to >50% at 66 h after transfection. Seventy-two hours after transfection, >90% cells showed outer membrane translocation of phosphatidylserine (Fig. 5B).

Discussion

The invasive character of malignant gliomas depends largely on the proteolytic destruction of the extracellular matrix. Several studies have indicated the involvement of proteases in tumor growth invasion and metastasis (13, 20). The involvement of uPAR and cathepsin B expression in aggressive gliomas suggests that they are important components of invasion and metastasis (3–5, 17, 21–24). Mitochondria are the central relaying stations that respond to both intracellular and extracellular signals in mediating caspase-dependent and caspase-independent cell death (25). Cytochrome *c* is an evolutionarily conserved water-soluble protein residing in the intermembrane space of the mitochondria. An electric potential ($\Delta\psi$) exists across the inner mitochondrial membrane, and, during mitochondrial-mediated cell death, this electric potential collapses and, in turn, releases cytochrome *c* into the cytosol (26).

In this study, we have shown that the down-regulation of uPAR and cathepsin B induces AIF nuclear translocation and partial caspase-dependent apoptosis (Fig. 6). We have previously shown that RNAi-mediated down-regulation of uPAR and cathepsin B leads to decreases in invasion, induction of angiogenesis, and tumor growth (18). This siRNA plasmid-mediated down-regulation of uPAR and cathepsin B efficiently down-regulates expression of the target gene(s). Of note, this down-regulation of uPAR and cathepsin B initiates a cascade of events involving the collapse of mitochondrial $\Delta\psi$ and subsequent release of cytochrome *c* into the cytoplasm. Cytochrome *c* in the cytoplasm combines with Apaf-1, caspase-9, and ATP to form the apoptosome (26).

In the present study, we observed an appreciable increase in the expression of activated caspase-9 and Apaf-1 in the formation of the apoptosome in pUC-treated cells (Apaf-1

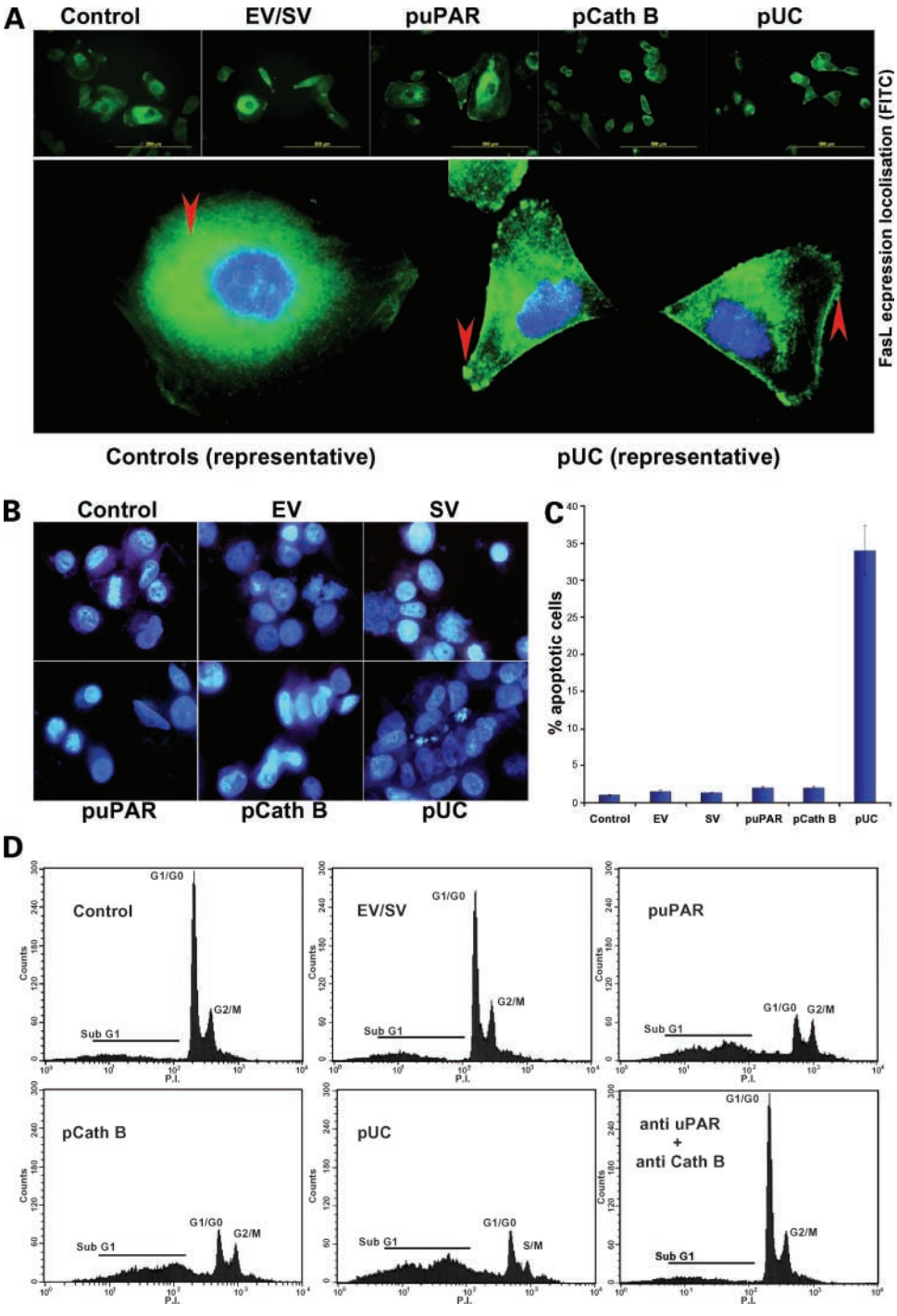

Figure 4. Immunolocalization of FasL and visualization of nuclear fragmentation in pUC-transfected SNB19 cells. SNB19 cells (1×10^4) were seeded on vitronectin-coated eight-well chamber slides, incubated for 24 h, and transfected with empty vector/scrambled vector, puPAR, pCath B, or pUC. After 72 h, cells were fixed with 3.7% formaldehyde and incubated with 1% bovine serum albumin in PBS at room temperature for 1 h for blocking. The slides were then washed with PBS, followed by the addition of IgG anti-FasL (mouse; 1:200). The slides were incubated at 4°C overnight and washed three times with PBS to remove excess primary antibody. Cells were then incubated with anti-mouse FITC conjugate (1:500 dilution) for 1 h at room temperature. The slides were then washed three times and covered with glass coverslips, and fluorescent photomicrographs were obtained for FITC. **A,** DAPI images were obtained where appropriate. SNB19 cells (1×10^4) were seeded on vitronectin-coated eight-well chamber slides, incubated for 24 h, and transfected with EV/SV, puPAR, pCath B, or pUC. After another 48 h, cells were fixed with 3.7% formaldehyde for 20 min at room temperature. The cells were then gently washed in PBS three times and incubated in 1 μg/mL RNase in PBS for 30 min. The cells were washed again gently, and a coverslip was mounted in DAPI-containing mounting media. **B,** DAPI fluorescence was visualized using a fluorescent microscope. **C,** the percentage of cells showing nuclear fragmentation was quantified as percent apoptotic cells. SNB19 cells (2×10^6) were seeded on vitronectin-coated plates and were either transfected with mock, empty vector, puPAR, pCath B, or pUC, or treated with antibodies for uPAR, cathepsin B, or both, and cultured for 48 h. Cells were trypsinized and treated with 50 μg/mL propidium iodide + 0.001% RNase A solution per standard protocols. The cells were then sorted on a fluorescence-activated cell sorter and quantified (10,000 cells sorted). **D,** effect of pUC on the cell cycle.

not shown), indicating cytochrome *c*–mediated activation of the apoptosome pathway (26). DFF40/CAD levels increased in pUC-treated cells compared with the controls. Detectable levels of DFF40/CAD were also seen in puPAR- and pCath B–treated cells. Increased expression of caspase-8 and caspase-9 in pUC-treated cells was also seen in pCath B–treated cells. Of note, there was no activation of caspase-3, the traditional effector caspase (25, 27). DFF40/CAD, which was activated in all three plasmid treated cells, on the other hand, has also been shown to be activated by caspase-3 and caspase-7 (28). This might indicate that DFF40/CAD is also activated by other caspases, such as caspase-8. Treatment of SNB19 cells with antibodies targeting uPAR and cathepsin B did not induce caspase-3, caspase-8, or caspase-9 but significantly decreased invasion as determined by the Matrigel invasion assay. Because

cathepsin B and uPAR are directly involved in invasion, inhibiting their activity with antibodies would retard invasion. The depletion of these molecules on the cell surface would achieve the same result, the difference being that the physical absence of uPAR and cathepsin B induced apoptosis. To determine whether there is a window of time when SNB19 glioma cells are still alive, and it is actually the effect of gene regulation/expression after pUC transfection that causes retardation in migration ability, we did the Annexin V assay to determine the outer cell surface translocation of phosphatidylserine. From the results, it is evident that at 60 h after transfection, >40% of the cells showed outer membrane translocation of phosphatidylserine. The translocation of phosphatidylserine increased to >50% at 66 h after transfection. Seventy-two hours after transfection, >90% of the cells showed outer membrane translocation of phosphatidylserine. For cells to migrate, cells need to alter the cytoskeleton and precisely control the expression of proteases towards the direction of migration in an extracellular matrix environment, and processes interfering with the expression of proteases or signaling molecules have the potential to alter the migration ability of cells. As has been shown, pUC-transfected cells fail to migrate 48 h after transfection, indicating that at 48 h, a majority of the cells had not been committed to apoptosis as determined by the Annexin V staining at 60 h where about 60% of the cells seemed to be ''normal.'' Seventy-two hours after transfection, it was observed that a majority of the transfected cells had committed to apoptosis (>90%), indicating that the most of the cells are alive up to

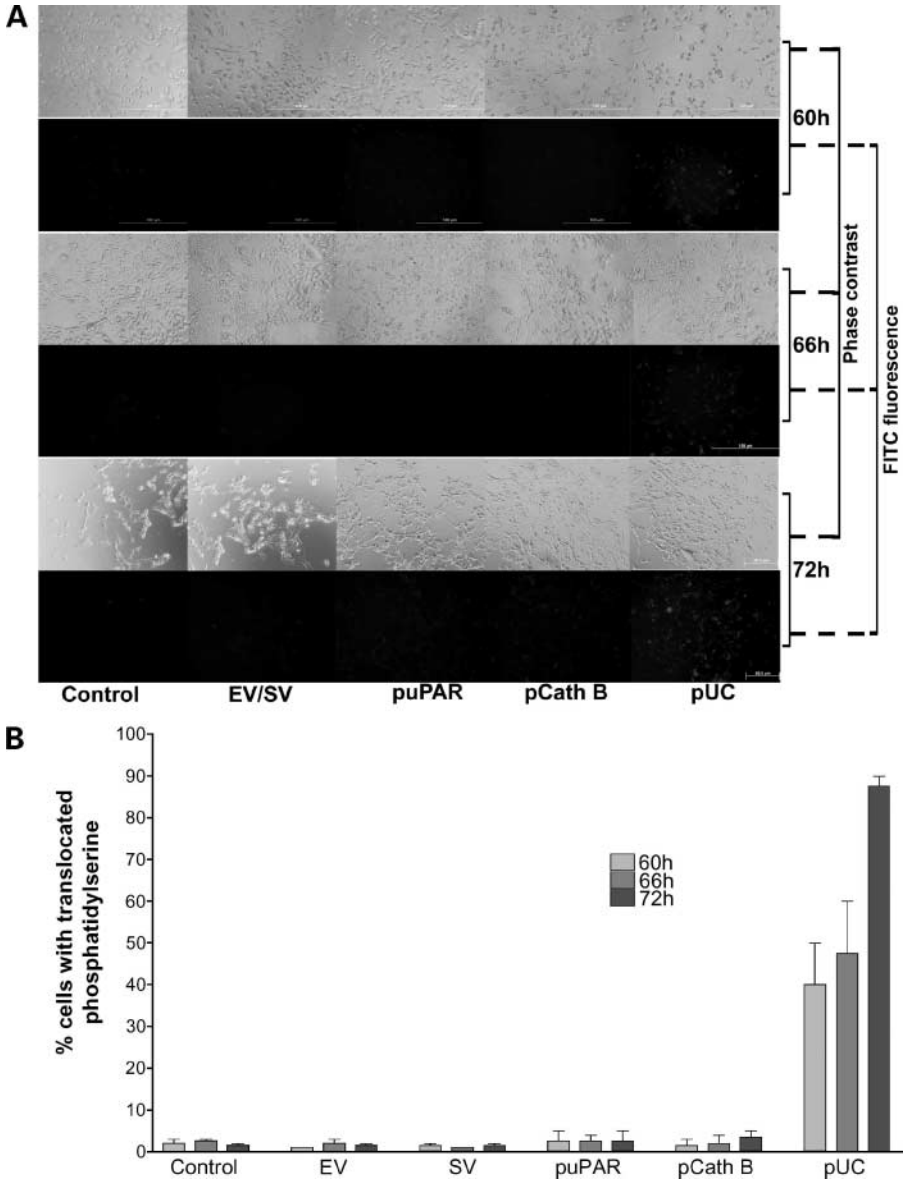

Figure 5. Determination of translocation of phosphatidylserine to the outer cell surface. To determine weather pUC-transfected cells were committed to the apoptotic pathway, SNB19 cells were transfected with control, empty vector, scrambled vector, puPAR, pCath B, or pUC, and the cell surface translocation of phosphatidylserine was determined by staining with FITC-conjugated Annexin V as described in Materials and Methods. Cells were observed under a fluorescence microscope using standard filter set for FITC. **A,** cells that have bound Annexin V-FITC were observed for green fluorescence in the plasma membrane. **B,** the fluorescent cells were counted and quantified as percentage of total cells as determined by phase-contrast microscopy.

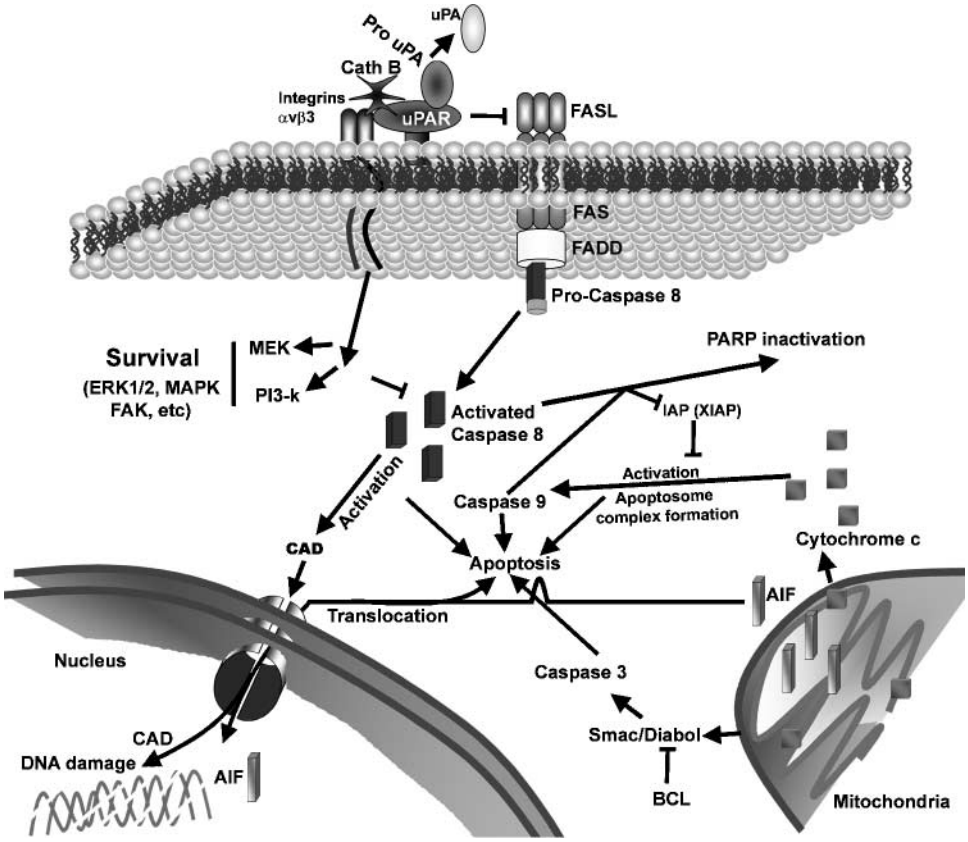

Figure 6. A schematic representation of the possible mechanism of action for apoptotic initiation via the involvement of mitochondria and cell surface receptors (uPAR and FasL receptor). The close proximity of integrins to FasL receptors might induce the activation of caspase-8, leading to a cascade of events, which eventually result in apoptosis.

72 h after transfection as observed by cell morphology, and that the decrease in migration is due to alteration in gene expression of various signaling molecules as discussed below.

XIAP, which belongs to family of apoptosis inhibitors (29), inhibits caspase activation. In the present study, we observed that pUC-treated cells showed a down-regulation of XIAP when compared with controls, thereby indicating some regulatory association with uPAR and cathepsin B. PARP cleavage was also detected in pUC-treated cells and is probably mediated via caspase-8 activation and in response to DNA damage. DFF40/CAD (30) cleavage of PARP resulted in nuclear DNA damage, indicating the activation of nucleases like AIF and EndoG (30). Here, AIF levels did not change, whereas nuclear translocation of AIF was observed, indicating the involvement of mitochondria in apoptosis. On the other hand, expression levels of FasL, which is similar to AIF, did not show any change in the total cellular content, but translocation to the cell membrane was observed. The binding of FasL to its receptor on the cell surface is known to initiate the activation of caspase-8, which is the extrinsic pathway for the initiation of apoptosis (31). In the present study, down-regulation of uPAR and cathepsin B by pUC initiated the activation of caspase-8 by >5-fold and, to a lesser extent, by the down-regulation of cathepsin B alone. Down-regulation of uPAR alone did not show activation of caspase-8 when compared with the controls.

uPAR is a glycosylphosphatidylinositol-anchored cell surface protein and is known to be associated with pro-uPA and cathepsin B (9); its close proximity to integrins has been implicated in its transmembrane signaling. uPAR also has binding sites for extracellular matrix components, such as vitronectin, and its association with cathepsin B could also possibly indicate its direct or indirect interaction with other cell surface proteins, such as Fas. The direct interaction between Fas and uPAR is not yet clear, but the uPAR-cathepsin B complex might inhibit or retard the translocation and binding of FasL to its receptor. It is not known whether the translocation of FasL to the cell surface is initiated by the down-regulation of uPAR and cathepsin B or whether the disruption in the molecular interaction of the uPAR complex with Fas is what causes FasL translocation. From the antibody studies here, where we blocked the activity of uPAR and cathepsin B with specific antibodies, no activation of caspase-8, caspase-3, or caspase-9 was observed. Interestingly, a decrease in invasion with antibodies was observed. This lack of activation may indicate that the molecular complex surrounding uPAR initiates a conformational change with Fas inhibiting caspase-8 activation. Antibodies were used to determine whether the presence of uPAR- and cathepsin B–inhibiting molecules, which retard invasion as seen in our results, also cause the induction of apoptosis as observed with the down-regulation of uPAR and cathepsin B on the cell surface.

It is very probable that the antibodies would be internalized; hence, no desired effect was observed. If the molecules in question are unavailable, we would expect a similar effect. Because uPAR is associated with other surface molecules, such as integrins, Annexin II, Tenacin-c, and seprase (9, 32–35), the internalization would involve this complex in whole or in part. Nonetheless, antibody treatment did not cause caspase-8 activation, and the use of antibodies did retard invasion as determined by the Matrigel invasion assay. In other words, because the use of antibodies for uPAR and cathepsin B did not result in the activation of caspase-8, the super molecular structure associated with uPAR and cathepsin B presumably near Fas retarded this activation. It is known that excess FasL or anti-Fas antibody extracellularly does initiate the extrinsic pathway of apoptosis by activating caspase-8. It would be logical to conclude that pUC-mediated down-regulation of uPAR and cathepsin B initiates the translocation of FasL extracellularly activating caspase-8 as seen by the immunocytochemical studies.

The nuclear translocation of AIF and the collapse of mitochondrial $\Delta\psi$ correlate well with each other in that the translocation of AIF would occur after the collapse in mitochondrial $\Delta\psi$ (36). The exact membrane permeabilization mechanisms, however, are still a matter of debate. Irrespective of the exact mechanism of membrane permeabilization, the antiapoptotic members of the Bcl-2 family tend to stabilize the barrier function of mitochondrial membranes, whereas proapoptotic Bcl-2 family proteins, such as Bax or Bak, tend to antagonize such function and permeabilize the mitochondrial membranes (37). Although the actual process of FasL regulation and activation still remains unclear, it can be concluded that the down-regulation of uPAR and cathepsin B activates FasL and induces its translocation to the cell surface as observed from our results. From the Western blot analysis, it is evident that DFF40/CAD is also activated indicating the involvement of caspases. The cleavage of PARP substantiates the activation of DFF40/CAD and is evidence for DNA damage. DAPI staining of pUC-transfected cells show evidence of nuclear damage. From our fluorescence-activated cell sorting analysis studies, pUC-transfected cells showed a large increase in the sub-G_1 population, indicating nuclear fragmentation and loss of nuclear indignity. In contrast, cells treated with antibodies for uPAR and cathepsin B did not show any change in population at the sub-G_1 stage and were similar to controls. Spatial-temporal expression and activation studies at the cellular level on proapoptotic molecules would give insight to the actual mechanisms involved in apoptosis. It is evident from this study that uPAR and cathepsin B participate in cellular mechanisms that are still unclear and may be involved in processes that are not fully understood in mediating apoptosis.

Our earlier survival studies, in which nude mice were implanted with intracranial SNB19 tumors and treated with plasmids expressing siRNA for uPAR and cathepsin B, showed retardation of tumor growth with no apparent apoptotic damage to the surrounding brain tissue (38). This mechanism of apoptosis via the down-regulation of uPAR and cathepsin B seems not to effect normal cells or cells that do not overexpress uPAR and cathepsin B. As such, uPAR and cathepsin B have potential as promising therapeutic agents. In conclusion, the down-regulation of uPAR and cathepsin B induces the nuclear translocation of AIF and the collapse of mitochondrial $\Delta\psi$ and causes the translocation of FasL to the cell surface, thereby activating caspase-8.

Acknowledgments

We thank Shellee Abraham for article preparation and Diana Meister and Sushma Jasti for article review.

References

1. Abe T, Mori T, Kohno K, et al. Expression of 72 kDa type IV collagenase and invasion activity of human glioma cells. Clin Exp Metastasis 1994;12:296 – 304.

2. Kinder DH, Berger MS, Mueller BA, Silber JR. Urokinase plasminogen activator is elevated in human astrocytic gliomas relative to normal adjacent brain. Oncol Res 1993;5:409 – 14.

3. Gladson CL, Pijuan-Thompson V, Olman MA, Gillespie GY, Yacoub IZ. Up-regulation of urokinase and urokinase receptor genes in malignant astrocytoma. Am J Pathol 1995;146:1150 – 60.

4. Rempel SA, Rosenblum ML, Mikkelsen T, et al. Cathepsin B expression and localization in glioma progression and invasion. Cancer Res 1994;54:6027 – 31.

5. Sivaparvathi M, Sawaya R, Wang SW, et al. Overexpression and localization of cathepsin B during the progression of human gliomas. Clin Exp Metastasis 1995;13:49 – 56.

6. Yamamoto M, Ueno Y, Hayashi S, Fukushima T. The role of proteolysis in tumor invasiveness in glioblastoma and metastatic brain tumors. Anticancer Res 2002;22:4265 – 8.

7. Mandal SK, Rao LV, Tran TT, Pendurthi UR. A novel mechanism of plasmin-induced mitogenesis in fibroblasts. J Thromb Haemost 2005;3:163 – 9.

8. Ravanti L, Kahari VM. Matrix metalloproteinases in wound repair. Int J Mol Med 2000;6:391 – 407.

9. Rao JS. Molecular mechanisms of glioma invasiveness: the role of proteases. Nat Rev Cancer 2003;3:489 – 501.

10. Cavallo-Medved D, Sloane BF. Cell-surface cathepsin B: understanding its functional significance. Curr Top Dev Biol 2003;54:313 – 41.

11. Podgorski I, Sloane BF. Cathepsin B and its role(s) in cancer progression. Biochem Soc Symp 2003;70:263 – 76.

12. Roberts LR, Adjei PN, Gores GJ. Cathepsins as effector proteases in hepatocyte apoptosis. Cell Biochem Biophys 1999;30:71 – 88.

13. Yan S, Sloane BF. Molecular regulation of human cathepsin B: implication in pathologies. Biol Chem 2003;384:845 – 54.

14. Go Y, Chintala SK, Mohanam S, et al. Inhibition of *in vivo* tumorigenicity and invasiveness of a human glioblastoma cell line transfected with antisense uPAR vectors. Clin Exp Metastasis 1997;15:440 – 6.

15. Mohan PM, Chintala SK, Mohanam S, et al. Adenovirus-mediated delivery of antisense gene to urokinase-type plasminogen activator receptor suppresses glioma invasion and tumor growth. Cancer Res 1999;59:3369 – 73.

16. Mohan PM, Lakka SS, Mohanam S, et al. Downregulation of the urokinase-type plasminogen activator receptor through inhibition of translation by antisense oligonucleotide suppresses invasion of human glioblastoma cells. Clin Exp Metastasis 1999;17:617 – 21.

17. Mohanam S, Chintala SK, Go Y, et al. *In vitro* inhibition of human glioblastoma cell line invasiveness by antisense uPA receptor. Oncogene 1997;14:1351 – 9.

18. Gondi CS, Lakka SS, Dinh DH, Olivero WC, Gujrati M, Rao JS. RNAi-mediated inhibition of cathepsin B and uPAR leads to decreased cell invasion, angiogenesis and tumor growth in gliomas. Oncogene 2004;23:8486 – 96.

19. Mohanam S, Sawaya R, McCutcheon I, Ali-Osman F, Boyd D, Rao JS. Modulation of *in vitro* invasion of human glioblastoma cells by urokinase-type plasminogen activator receptor antibody. Cancer Res 1993;53:4143 – 7.

20. Koop S, Khokha R, Schmidt EE, et al. Overexpression of metalloproteinase inhibitor in B16F10 cells does not affect extravasation but reduces tumor growth. Cancer Res 1994;54:4791 – 7.

21. Demchik LL, Sameni M, Nelson K, Mikkelsen T, Sloane BF. Cathepsin B and glioma invasion. Int J Dev Neurosci 1999;17:483 – 94.

22. Mikkelsen T, Yan PS, Ho KL, Sameni M, Sloane BF, Rosenblum ML. Immunolocalization of cathepsin B in human glioma: implications for tumor invasion and angiogenesis. J Neurosurg 1995;83:285 – 90.

23. Strojnik T, Kos J, Zidanik B, Golouh R, Lah T. Cathepsin B immunohistochemical staining in tumor and endothelial cells is a new prognostic factor for survival in patients with brain tumors. Clin Cancer Res 1999;5:559 – 67.

24. Yamamoto M, Sawaya R, Mohanam S, et al. Expression and localization of urokinase-type plasminogen activator receptor in human gliomas. Cancer Res 1994;54:5016 – 20.

25. Cregan SP, Dawson VL, Slack RS. Role of AIF in caspase-dependent and caspase-independent cell death. Oncogene 2004;23:2785 – 96.

26. Hajra KM, Liu JR. Apoptosome dysfunction in human cancer. Apoptosis 2004;9:691 – 704.

27. Meng XW, Fraser MJ, Feller JM, Ziegler JB. Caspase-3 activates endo-exonuclease: further evidence for a role of the nuclease in apoptosis. Apoptosis 2000;5:243 – 54.

28. Semenov DV, Aronov PA, Kuligina EV, Potapenko MO, Richter VA. Oligonucleosome DNA fragmentation of caspase 3 deficient MCF-7 cells in palmitate-induced apoptosis. Nucleosides Nucleotides Nucleic Acids 2004;23:831 – 6.

29. Harada H, Grant S. Apoptosis regulators. Rev Clin Exp Hematol 2003; 7:117 – 38.

30. Hong SJ, Dawson TM, Dawson VL. Nuclear and mitochondrial conversations in cell death: PARP-1 and AIF signaling. Trends Pharmacol Sci 2004;25:259 – 64.

31. Costelli P, Aoki P, Zingaro B, et al. Mice lacking TNFalpha receptors 1 and 2 are resistant to death and fulminant liver injury induced by agonistic anti-Fas antibody. Cell Death Differ 2003;10:997 – 1004.

32. Xue W, Mizukami I, Todd RF III, Petty HR. Urokinase-type plasminogen activator receptors associate with beta1 and beta3 integrins of fibrosarcoma cells: dependence on extracellular matrix components. Cancer Res 1997;57:1682 – 9.

33. Dumler I, Weis A, Mayboroda OA, et al. The Jak/Stat pathway and urokinase receptor signaling in human aortic vascular smooth muscle cells. J Biol Chem 1998;273:315 – 21.

34. Artym VV, Kindzelskii AL, Chen WT, Petty HR. Molecular proximity of seprase and the urokinase-type plasminogen activator receptor on malignant melanoma cell membranes: dependence on beta1 integrins and the cytoskeleton. Carcinogenesis 2002;23:1593 – 601.

35. Mahdi F, Shariat-Madar Z, Todd RF III, Figueroa CD, Schmaier AH. Expression and colocalization of cytokeratin 1 and urokinase plasminogen activator receptor on endothelial cells. Blood 2001;97: 2342 – 50.

36. Otera H, Ohsakaya S, Nagaura ZI, Ishihara N, Mihara K. Export of mitochondrial AIF in response to proapoptotic stimuli depends on processing at the intermembrane space. EMBO J 2005;24: 1375 – 86.

37. Cory S, Adams JM. The Bcl2 family: regulators of the cellular life-or-death switch. Nat Rev Cancer 2002;2:647 – 56.

38. Gondi CS, Lakka SS, Dinh D, Olivero W, Gujrati M, Rao JS. Downregulation of uPA, uPAR and MMP-9 using small, interfering, hairpin RNA (siRNA) inhibits glioma cell invasion, angiogenesis and tumor growth. Neuron Glia Biology 2004;1:165 – 76.